

# Analysis of data from full-scale prototype testing of the WASP - A novel wave measuring buoy.

Brendan Walsh, Thomas Kelly, Robert Carolan, Mark Boland, Thomas Dooley.

**Abstract—** To assess the viability of locations for wave energy farms, and design effective coastal protection measures, knowledge of local wave regimes is required. Current regime-measuring devices are expensive, and the aim of the WASP Project is to develop a low-cost, self-powering wave-measuring device. The Wave-Activated Sensor Power Buoy (WASP) comprises a floating body with a moonpool. The relative motion of the water level in the moonpool to the buoy will pressurise and depressurise the air above the water column. It has previously been demonstrated through the tank testing of scale-models that the incident wave spectrum may be estimated from measurements of the pressure within the air above the water column [1]. A full scale prototype of the WASP was assembled and deployed in February 2019. The purpose of the prototype was to determine if a relationship between the incident wave spectrum and the pressure spectrum within an oscillating water column (OWC) chamber with a view to estimating sea-states at full-scale. This paper seeks to validate the use of measurements taken of the pressure in a volume of air contained in a chamber above an oscillating water column (OWC) (which is in communication with the ocean) to estimate the sea state which induces motion of the water column. The process by which a sea state may be estimated shall be presented along with data and typical results.

**Keywords—** Oscillating water column, Prototype design, Wave measurement, wave spectra.

## I. INTRODUCTION

Measurement of ocean waves plays a crucial role in understanding and determining wave energy resources for example to assess the viability of locations for wave energy farms, and design effective coastal protection measures, knowledge of local wave regimes is required. While it may be possible to estimate expected waves at various locations, actual field measurements are required to both validate these estimates as well as offer data on the

sea state at a location where an accurate model may not be easily constructed [1]. There are various systems and methods available for measurement. These include Seabed pressure sensors, acoustic current profilers. Radar (land based and satellite) and surface following buoys.

The work described in this paper has been undertaken as part of a phased project with the aim of developing a low-cost, wave-powered buoy to measure wave conditions to meet the needs of both developers and local authorities, christened the Wave Activated Sensor Power Buoy (WASP). A number of such low-cost buoys may potentially be deployed at a location to measure the local wave climate both temporally and spatially. Scale model tank testing was carried out on the concept as described in ‘*Scale Model Testing of the WASP – a Novel Wave Measuring Buoy*’, M. Boland. 2019, while the prototype full-scale device was described in ‘*The Design and Construction of a Prototype WASP - a Novel Wave Measuring Buoy*’, R. Carolan. 2019.

The WASP comprises a floating body with a central moonpool. The relative motion of the water level in the moonpool to the buoy will pressurise and depressurise the air above the water column. Air flows generated by the change in pressure will, in the final design of the device, be used to drive a unidirectional turbine in the manner of an oscillating water column, which, in turn, will be used in conjunction with a generator to recharge an on-board battery pack. It is intended that, once the WASP has been suitably calibrated, the wave spectrum may be estimated from measurements of the pressure of the air above the water column by determining a relationship between the incident wave spectrum and the pressure spectrum within the OWC chamber. Important statistical parameters relating to the sea-state, such as the significant wave height, zero-cross period etc. may then be estimated from the spectral moments of the estimated wave spectrum. Mathematical techniques may be used to determine sea-

©2023 European Wave and Tidal Energy Conference. This paper has been subjected to single-blind peer review.

This work was funded by the National Infrastructure Access Programme administered by the Marine Institute of Ireland under grant no. NIAP - LS - 16010.

B. Walsh is with the Dundalk Institute of Technology, Dundalk, Ireland (e-mail: brendan.walsh@dkit.ie).

R. Carolan is with the Dundalk Institute of Technology, Dundalk, Ireland (e-mail: robert.carolan@dkit.ie).

M. Boland was with Dundalk Institute of Technology, Dundalk, Ireland (e-mail: mboland11@gmail.com).

T. Kelly is with Dundalk Institute of Technology, Dundalk, Ireland (e-mail: kellyt@dkit.com).

T. Dooley was with the Dundalk Institute of Technology, Dundalk, Ireland (e-mail: thomas.dooley@dkit.com).

Digital Object Identifier: <https://doi.org/10.36688/ewtec-2023-481>

states from the time series of the air pressure. Such techniques could include inverse transfer functions, neural networks and numerical estimators. The WASP concept has been investigated through tank testing of a 1:20 scale model [2]. The initial full-scale prototype of the WASP uses a modified, off the- shelf buoy, the ‘*Seagull*’ navigation buoy manufactured by JFC Manufacturing Company Ltd., Ireland [3], and was tested at the BlueWise Marine Marine and Renewable Energy test site off the West coast of Ireland [4]. The purpose of the prototype was to obtain data to develop the process of using the pressure time series to estimate sea-state parameters in the real world at full scale. To this end, the device was deployed at a location where the wave regime is independently measured by a Waverider surface following buoy at the BlueWise Marine test site. The prototype is not wave powered, and the air chamber above the water column is intentionally sealed from atmosphere, in order to maximise pressure in the chamber. It should be noted that the ‘*Seagull*’ buoy is not generally intended to be deployed in this configuration.

## II. THEORY

Of the various methods listed above, the current work focuses on the inverse transfer function method. Consider the single-input, single output (SISO) system in Figure 1.

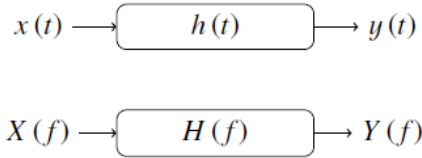


Fig. 1. A single input/output system in the time domain and the frequency domain.

$x(t)$  represents the stationary input

$y(t)$  represents the output

$h(t)$  represents the impulse response of the system

$X(f)$  represents the Fourier transform of  $x(t)$

$Y(f)$  represents the Fourier transform of  $y(t)$

$H(f)$  is the frequency-dependent, Fourier transfer function between  $X(f)$  and  $Y(f)$

$H(f)$  is the Fourier transform of  $h(t)$ .

The two-sided, autospectral density function,  $S_{xx}(f)$  for an input time signal  $x(t)$  is related to the autospectral density function,  $S_{yy}(f)$  for an output signal  $y(t)$  by:

$$S_{yy}(f) = |H(f)|^2 S_{xx}(f) \quad (1)$$

In the work described herein, the measured time series of air pressure in the OWC is the input signal  $x(t)$  and the time series of surface water elevation of the incident sea state is the output signal  $y(t)$ . The two-sided auto-spectral density functions of the pressure data from the prototype WASP and the measured incident wave height data from

the Waverider buoy, are  $S_{xx}(f)$  and  $S_{yy}(f)$  respectively. Thus the squared magnitude of the transfer function between the pressure in the prototype WASP OWC and the incident sea state can be derived from [5]:

$$|H(f)|^2 = \frac{S_{yy}(f)}{S_{xx}(f)} \quad (2)$$

## III. PROTOTYPE DEPLOYMENT AND PERFORMANCE

The prototype was deployed in February 2019 at the Marine Institute Galway Bay observatory, and successfully recorded and transmitted data daily until its recovery in June 2019, see figure 2. The WASP was moored



Fig. 2. The WASP deployed at the Marine Institute Galway Bay observatory, Ireland, 2019

at a single point to a previously established single mooring system specifically placed for the WASP. The test site is located approximately 1.2 kilometres off the Spiddal coastline in Galway bay, and approximately 400 metres from the location of the existing Irish Marine Institute Waverider data buoy, see Figure 3.

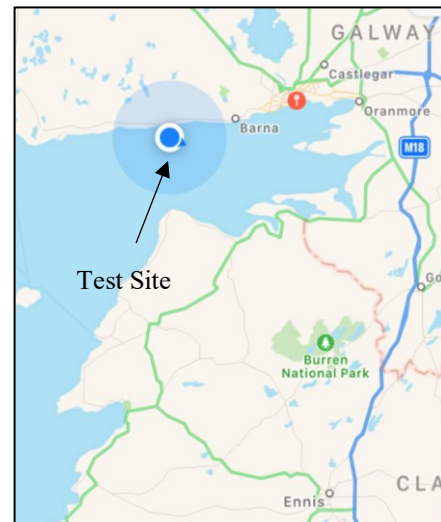


Fig. 3. Test site location at the Marine Institute Galway Bay observatory, Ireland.

The test site allows for less exposed trials of smaller scale ocean energy devices, and those at an earlier stage of development. Conventional wave regime measurement buoys work by ‘following’ the free surface of the ocean [6]. On-board accelerometers measure the acceleration of the buoy, and the displacement of the buoy is then determined from the double integration of the accelerometer data. Hence, the time series of the motion of the buoy can be obtained by assuming the motion of the buoy matches the free surface elevation and the wave spectrum at the deployment site may be estimated. Unlike wave-following buoys, the operational principle of the WASP depends on the interaction of the WASP with the ocean waves in order to pressurise and depressurise the air above the water column, the WASP does not operate on a wave-following basis. The air chamber above the water column in the prototype WASP is sealed. The time series of the pressure in the air volume above the water column is measured and recorded and sampled at 8Hz. The WASP was retrieved in July 2019 having successfully uploaded 24 hours of uninterrupted data each day for the duration of the deployment. During the deployment, the WASP was subject to a wide range of weather and sea state conditions and from a robustness perspective had survived and subsequently recorded data from the most severe winter storms of that year, including storms Gareth and Hannah, both of which brought gusts in excess of 130km/h. The deployment resulted in the acquisition of several months of pressure signal readings from two Keller piezo-resistive, differential pressure sensors. Of these sensors, one covers low range at high sensitivity  $\pm 200$  millibar. The other at  $\pm 1$  bar for normal operation precision and extreme pressure events. An example of a typical pressure recording for one day is shown below in figure 4 from both the 200mbar and 1 bar pressure sensors.

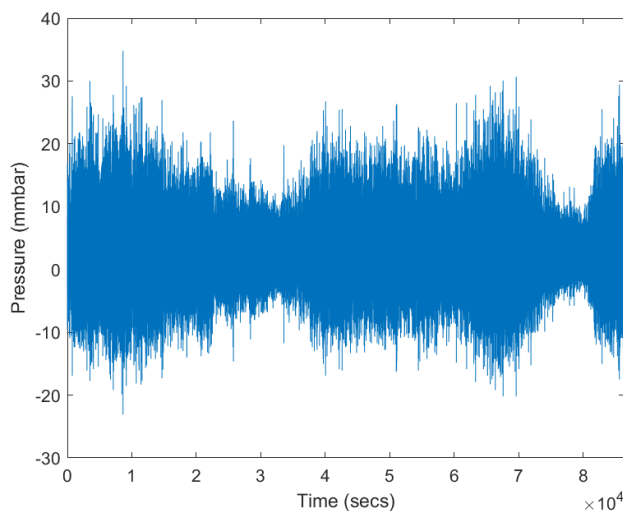


Fig. 4. Pressure/time graphical output (03.03.19)

The battery performance and air temperature (within the daymark where the batteries and data management system were stored) over a 24 hours period can also be monitored with examples shown in Figures 5 and 6 below. While battery and temperature monitoring may not be useful for wave estimation, the information is useful to monitor the WASP's performance. It is interesting to note in Figure 5, this was a relatively overcast day, and as the cloud covering cleared one can note an increase in voltage. Similarly, in Figure 6, one can see the change in temperature as the day progresses. There were no issues with regard to temperature throughout the duration of deployment, ranging from 10°C to 30°C which is a comfortable operating range from an electronics point of view.

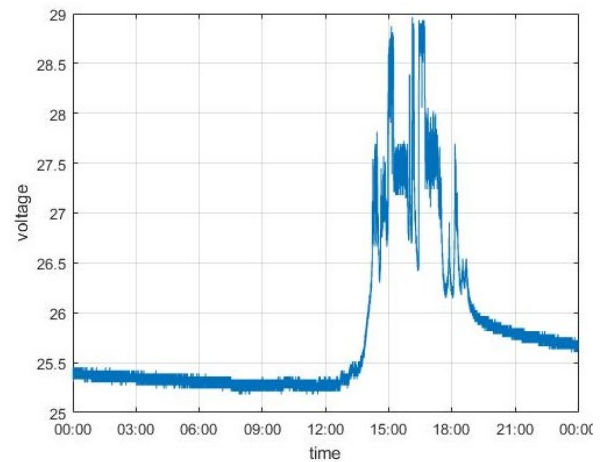


Fig. 5. Battery performance over 24 hours (03.03.19)

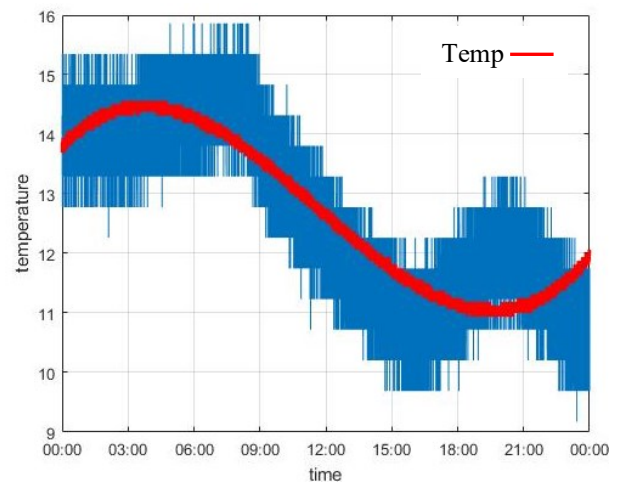


Fig. 6. Temperature (degrees Celsius) over 24 hours (03.03.19)

#### IV. PROCESSING AND DATA ANALYSIS

Data was uploaded from the WASP to Microsoft Azure cloud service daily via 4G (LTS) module from Digital yacht [7], from the prototype WASP buoy. While data from the corresponding Waverider buoy at the BlueWise Marine test site was provided by the Marine Institute Ireland.

To date, three approaches have been explored to analyse the data obtained from the WASP prototype during the deployment outlined above, with the final approach

appearing to demonstrate the viability of using such pressure measurements to estimate key statistical parameters in real-world situations.

The first analysis approach involved a comparison between the sea-state parameters  $H_s$  (significant wave height) and  $T_z$  (zero up-cross period) obtained from the existing data buoy, and corresponding parameters obtained from the spectral moments of the single-sided pressure density spectrum obtained from the WASP.

Waverider data was acquired in half hour samples. The time series data was not available to the authors. The Marine Institute waverider data time stamp is given as an unsigned number representing the number of seconds elapsed after 1 Jan 1970 in UTC time and in this regard, the correct timing had to be interpreted if an accurate comparison was to be drawn. The WASP data was also processed into half hour samples and it was important to ensure that the two time series were indeed coincident. The prototype WASP time series pressure data was transformed to the frequency domain using Welch's Method [8] in order to generate a power density spectrum (PDS), obtain the spectral moments and in turn estimate what was termed '*pseudo*'  $H_s$  and  $T_z$  values for a specific half hour sample. The energy density spectrum was found for a half hour sample of the WASP pressure signal using Welch's method, the spectral moments were found and in turn '*pseudo*'  $H_s$  and  $T_z$  values. All of the Waverider  $H_s$  and  $T_z$  values were collated and similar sea-state events identified on varying dates. It was assumed that the incident wave spectrum experienced by the waverider was identical to that experienced by the WASP. It should be noted that the two devices were located approximately 400m apart within the observatory for the duration of the deployment. The power density spectra were generated for the Waverider for specific half hour samples and in turn the corresponding WASP spectra for the coinciding half hour in order to generate associated spectral moments and sea-state parameters.

A comparison was carried out between all Waverider and WASP '*pseudo*'  $H_s$  and  $T_z$  values for the a single month. The two sets of values for each device were plotted against one another and fitted a least squares regression to the output. A poor  $R^2$  correlation in the order of 0.6 was observed between  $H_s$  values and an  $R^2$  correlation in the order of 0.3 observed between the  $T_z$  values. With poor correlation observed using this simplified comparison approach an alternative analysis route was explored.

In the second analysis approach, described in previous EWTEC paper '*Full-scale Prototype Testing of the WASP – A Novel Wave Measuring Buoy*', B. Walsh. 2021, the prototype WASP time series pressure data was converted to the frequency domain (again using Welch's method) and used in conjunction with provided incident wave spectra from the Waverider buoy to estimate the magnitude of the linear transfer function between the incident wave spectra at the

existing buoy location and the pressure spectrum from the WASP. However, no single half-hour data set from the existing buoy included information at all the required frequencies (ranging from 0 to 1 Hz). Thus, a composite transfer function was generated whereby different half hour data sets were used to obtain the transfer functions over different frequency ranges. The magnitude of transfer functions were established for ranges of frequencies between (0.0 and 0.4Hz, 0.4 and 0.6Hz and 0.6 and 1.0Hz) using different half hour sea states and then combined to obtain the magnitude of a transfer function that was used to estimate all half hour sea states based on the pressure signal from the WASP. Plots of estimate wave spectra were generated alongside measured incident wave spectra.

Using the magnitude of transfer function thus obtained between the pressure in the Prototype WASP OWC and the surrounding sea-state has produced some good estimations across three frequency ranges for similar wave spectra to those used to generate the squared magnitudes of the transfer function. However, some caveats do exist:

- . There are issues with the individual squared transfer functions up to 0.1Hz involving lack of information and anomalous peaks.
- . Estimations with spectral densities up to 0.05m<sup>2</sup>/Hz are producing anomalous peaks and troughs at various frequencies across all three functions.
- . The squared magnitude of transfer functions for frequencies up to 0.4Hz are more accurate due to being information rich.

There are non-linearities in the estimations which manifest as anomalous peaks and troughs suggesting there are issues in the prototype design or the acquisition of data. It is known that on deployment a number of openings were discovered in the OWC which were sealed insitu. The possibility of air passing from the chamber and affecting pressure readings can not be discounted. The combined squared transfer function exhibits too variable results to be considered reliable. This is due to the balance of information richness and spectral energy being in the 0Hz to 0.4Hz range. In this regard, a third alternative analysis route was explored.

In the third analysis approach, Power density spectra were generated for all c.6,000 half-hour samples for the Waverider device. A typical Waverider half hour sample power density spectrum is presented in Figure 7 below.

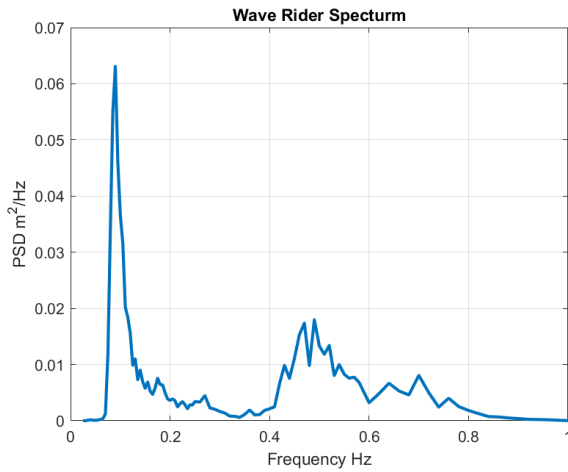


Figure 7 - Waverider Spectrum for 10<sup>th</sup> April 04:00-04:30  
Hs 0.3m and Tz 2.39s

Power density spectra for the corresponding half hour samples of the WASP were then generated. A typical Wasp device half hour sample power density spectrum is presented in Figure 8 below.

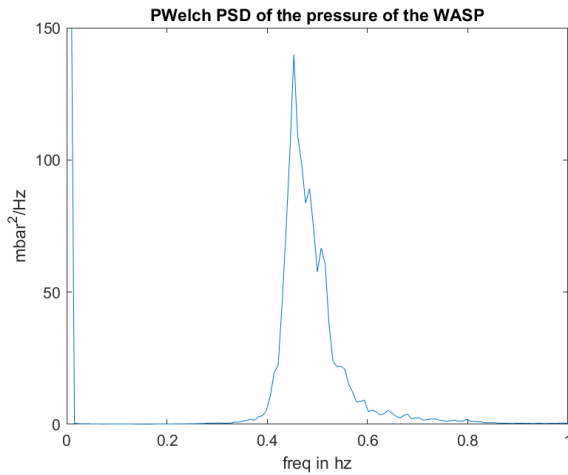


Figure 8 - Wasp pressure Spectrum for 10<sup>th</sup> April 04:00-04:30

A linear transfer function, based on Equation (2), between the WASP and the Waverider data was then produced for the entire month of March 2019 and an average transfer function formed. See figures 9 and 10 below.

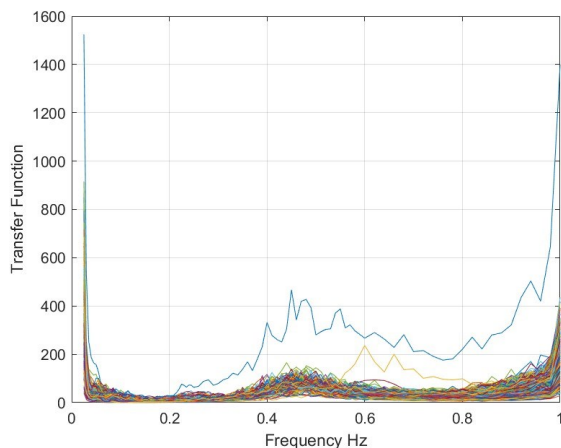


Fig.9. All transfer functions for month of March 2019

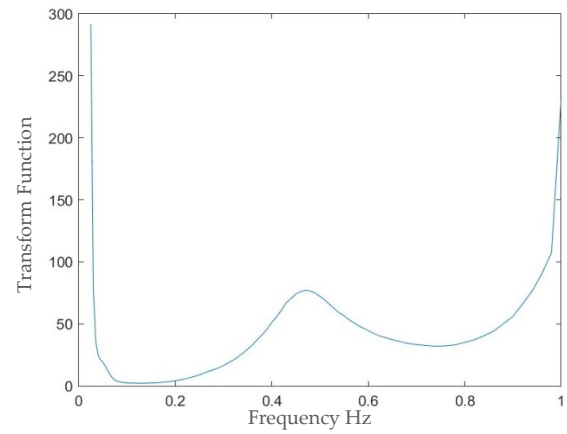


Fig.10. Average transfer function for month of March 2019

## V. RESULTS

Waverider data is acquired in half hour samples. The incident wave data is reported by the existing data buoy for a range of frequencies between 0 and 1.0Hz.

All data from the month of March was used as training data to produce the transfer function while the remaining data for the months of April, May and June used as validation data.

The March transfer function was applied to the WASP data for April, May and June to generate an estimated wave spectrum for each half-hour data segment. Spectral moments were then derived for the WASP and the Waverider, which were used to estimate  $H_s$  and  $T_z$  for every half hour sample for both devices for each month. Figures 11, 12 and 13 present a comparison between spectra from the WASP and the Waverider for single half hour samples using the above approach on randomly selected half hour samples.

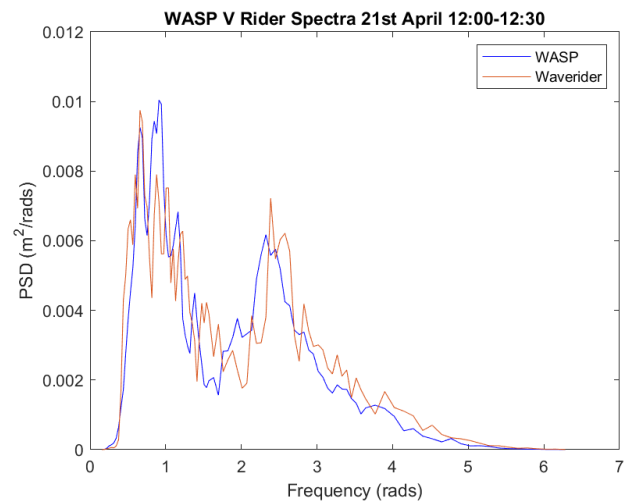


Fig.11. Wasp V Rider spectra for 21<sup>st</sup> April 12:00-12:30  
Rider: Hs = 0.404m and Tz = 3.41secs  
Wasp: Hs = 0.398m and Tz = 3.30secs



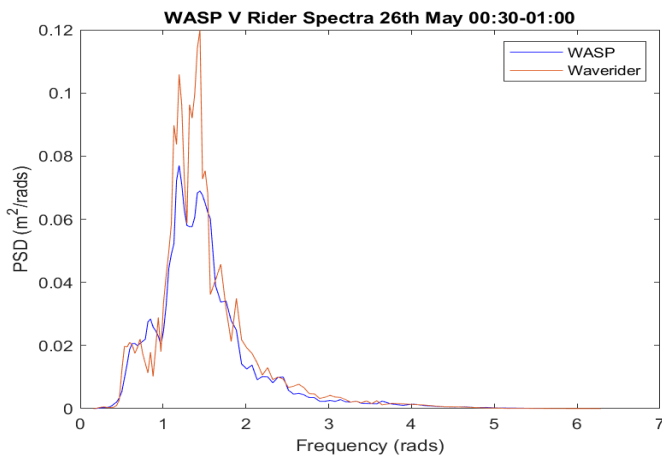


Fig. 12. Wasp V Rider spectra for 26<sup>th</sup> May 00:30-01:00  
Rider:  $H_s = 1.04\text{m}$  and  $T_z = 4.29\text{secs}$   
Wasp:  $H_s = 0.90\text{m}$  and  $T_z = 4.11\text{secs}$

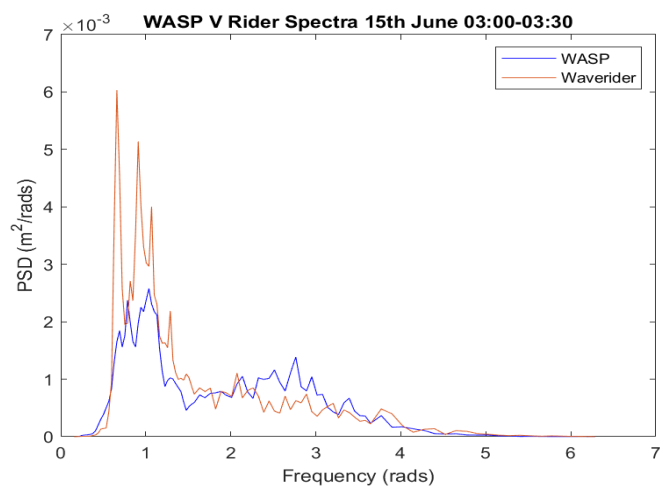


Fig. 13. Wasp V Rider spectra for 15<sup>th</sup> June 03:00-03:30  
Rider:  $H_s = 0.23\text{m}$  and  $T_z = 4.3\text{secs}$  Wasp:  $H_s = 0.17\text{m}$  and  $T_z = 3.35\text{secs}$

Having produced spectral moments,  $H_s$  and  $T_z$  were for all half hour samples for the months of April, May and June with 98% correlation for both parameters in all cases. Figures 14, 15 and 16 present all Wasp and Waverider  $H_s$  values for the entire months of April, May and June respectively.

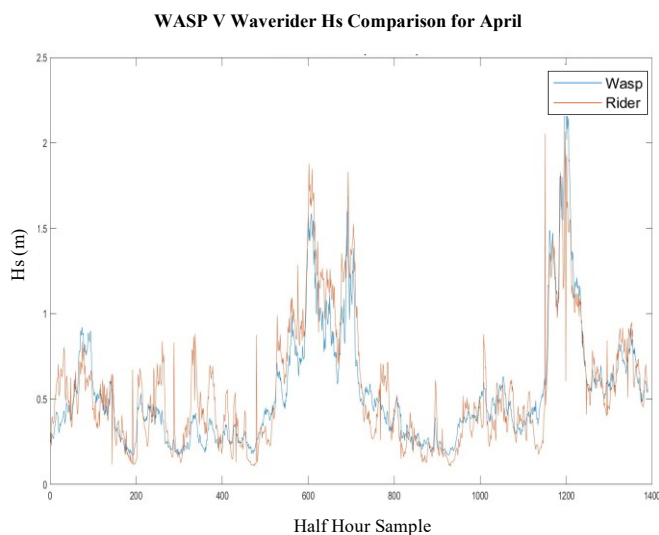


Fig. 14. Wasp V Rider Hs values for April 2019

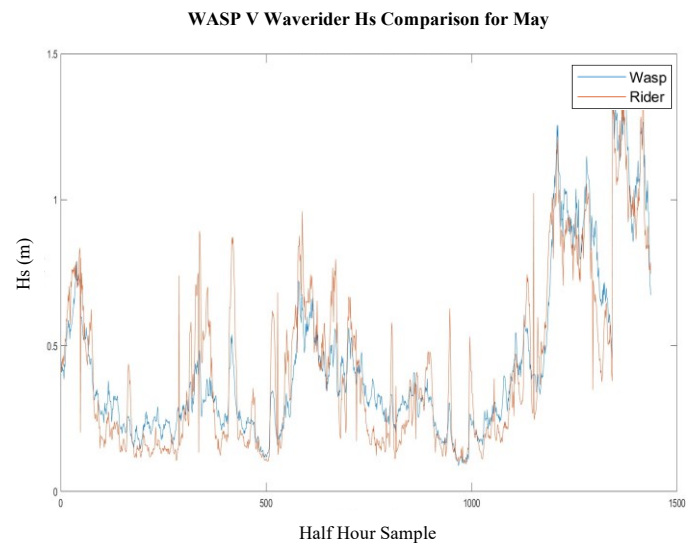


Fig. 15. Wasp V Rider Hs values for May 2019

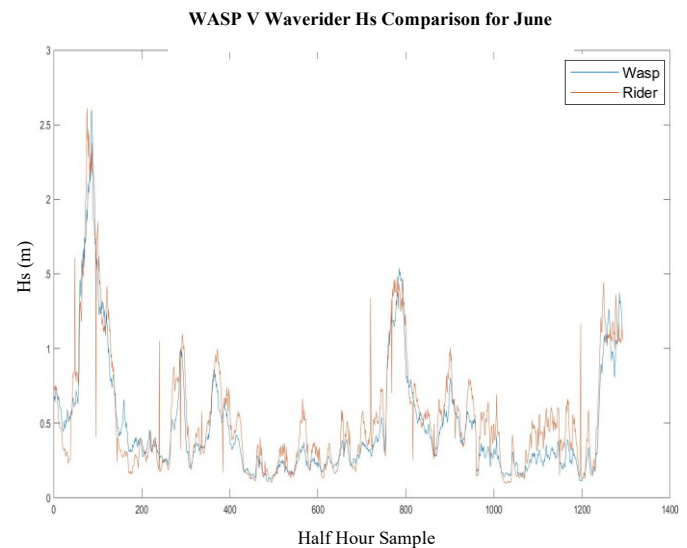


Fig. 16. Wasp V Rider Hs values for June 2019

Figures 17, 18 and 19 present all Wasp and Waverider  $T_z$  values for the entire months of April, May and June respectively.

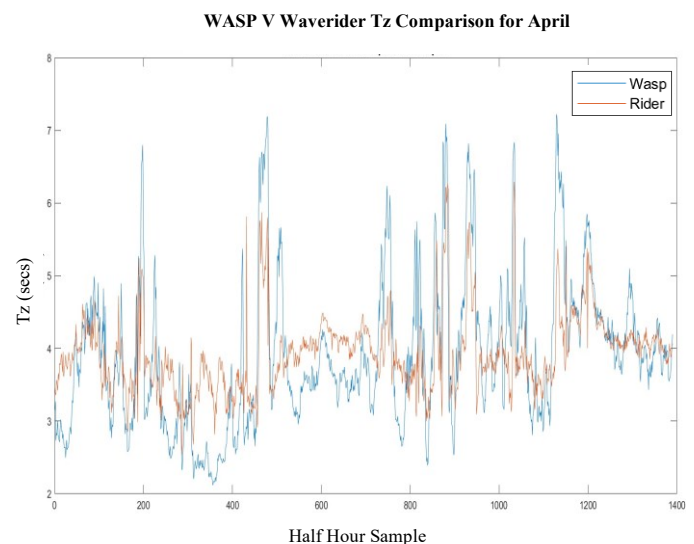


Fig. 17. Wasp V Rider Tz values for April 2019

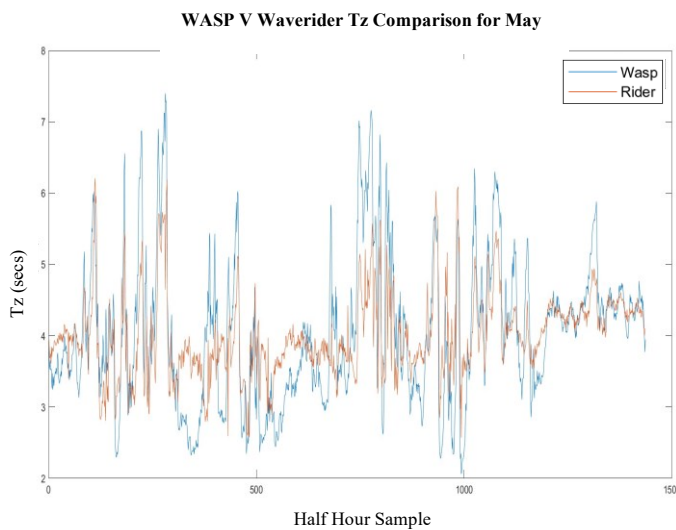


Fig. 18. Wasp V Rider Tz values for May 2019

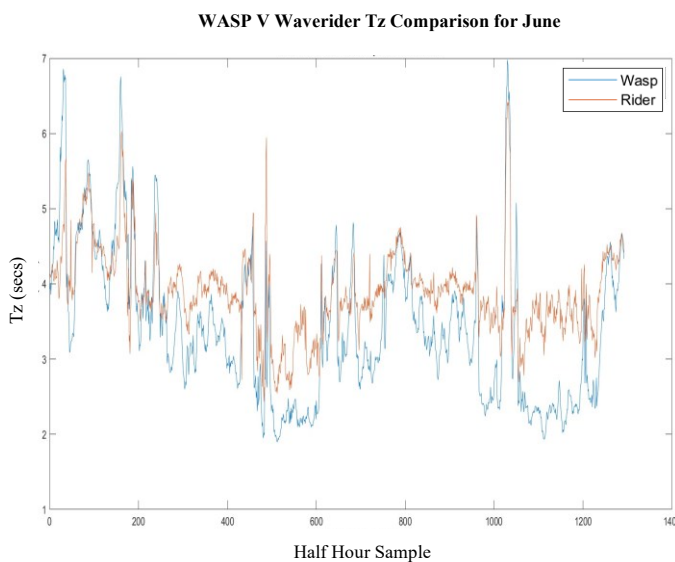


Fig. 19. Wasp V Rider Tz values for June 2019

As can be seen, initial analysis of the data established that good information is present, however work is still ongoing. The authors acknowledge that there are other methods yet to be explored as mentioned previously, as the linear transfer function does have some limitations.

## VI. CONCLUSION

The initial results from the third and current round of analysis are positive with correlation between spectra and  $H_s$  and  $T_z$  values in the order of 98% and it is now proposed to continue along this approach.

In some instances, the WASP  $H_s$  and  $T_z$  values appear to be higher than the Waverider and vice versa, this may be due to the use of an average transfer function drawing the higher values down and the lower values up.

## VII. FURTHER WORK

In further work, in order to ensure no seasonal bias occurs by using March data only as training, it is proposed to take 50% of a randomly chosen selection of data over the

four months and use as training data with the remaining data over the four months for testing.

In order to further refine the capabilities of the WASP to estimate sea-states, it is proposed to use the root mean squared (RMS) of the pressure signals to tailor specific transfer functions to corresponding sea states. Processed together the results are non-linear, however taking a series of smaller linear sections could lead to higher levels of accuracy in measuring sea-states by the WASP with specific transfer functions being applied to appropriate pressures.

Consideration will also be given to the redesign of the WASP to broaden frequency responses of the buoy and the OWC and therefore increase the information richness over a larger frequency range for generating squared transfer functions.

Employ Inertial Measurement Units (IMUs) to establish transfer functions between incident waves and the buoy motion to assist with the first recommendation.

Install wave probes in the OWC chamber to investigate sloshing mode.

Following on from successful completion of Phase 1 (subject of previous NIAP funding) and proof of concept, in Phase 2 (subject to recent NIAP funding qualification), the Technology Performance Level will be increased with the main objective to further reduce the cost of the WASP while also reducing the power consumption. Phase 2 deployment is scheduled for late of 2023.

This shall be achieved through development of low cost custom made electronic components as opposed to more expensive off the shelf devices and to draw comparisons between the wave field estimated from the more expensive pressure signal model in Phase 1 and the wave field estimated from on board accelerometers as proposed as part of Phase 2 future work. The required capital and operational costs of the WASP shall be an order of magnitude less expensive than similar technologies.

Phase 3 (to be funded through the OceanDemo scheme) will concentrate on further project work which envisages the addition of a Wells turbine to self-power the buoy.

## ACKNOWLEDGEMENT

The Authors would like to acknowledge the assistance provided in preparing the prototype WASP device for deployment by The BlueWise Marine, Marine and Renewable Energy test site, Co. Galway, Ireland, and by JFC Ltd, Tuam, Co. Galway. Finally, the authors acknowledge the assistance given by the staff of P&O Maritime, who also provided the solar panels and associated regulators used in this project.

## REFERENCES

- [1] Arthur Percher. Hand book on Ocean Energy. SpringerOpen. 2016

- [2] M Boland "Scale model testing of the WASP – a novel wave measuring Buoy" presented at European Wave and Tidal Energy Conference, Napoli, Italy, 2019.
- [3] JFC Marine, Ireland [Online]. Available: <https://www.jfcmarine.com>
- [4] BlueWise Marine, Ireland [Online]. Available: <https://www.marine.ie>
- [5] S. Bendat and A. G. Piersol, Random Data: Analysis and Measurement Procedures. New York: Wiley, 2011.
- [6] Datawell, Netherlands [Online]. Available: <https://www.datawell.nl/Products/Buoys/DirectionalWaverider/MkIII.aspx>
- [7] Digital Yacht, United Kingdom. [Online]: Available: <https://digitalyacht.co.uk/product/4g-connect/>
- [8] P.D. Welch, "The use of fast Fourier transform for the estimation of power spectra: A method based on time averaging over short, modified periodograms". IEEE Transactions on audio and Electroacoustics - vol. 15 pp 70-73, 1967.